Study of Passive Magnetic Bearings for Vertical-Axis Wind Turbines

Elkin F. Rodriguez*
Universidade Federal do Rio de Janeiro
Rio de Janeiro, Brazil

Richard M. Stephan
Universidade Federal do Rio de Janeiro
Rio de Janeiro, Brazil

Abstract

The increasing world energy demand as well as the necessity of environmental clean developments has turned the industry attention to improvements in renewable energy. In this context, wind power plants present technological advantages as an excellent source of clean energy.

The current vertical-axis wind turbines are going to be a novel energy supplier in urban centers due to both low-cost and low-impact architectural design. Moreover, they have good performance even in the presence of turbulent winds. A magnetic suspension can greatly improve the performance, expanding the operating points to very low wind velocities.

Active magnetic bearings present limiting factors such as power consumption and complexity of the system, due to sensors, power electronic circuits and the control system. In other way, passive techniques, which use permanent magnets and/or superconductors, can be alternatives in some applications.

This paper presents a contribution to the design of passive magnetic bearings for vertical-axis wind turbines. Finite element simulations and experimental data will be presented.

1 Introduction

Magnetic Bearings have gained importance in industrial applications, as they allow operation without contact between moving and fixed parts, overcoming the limitations found in mechanical bearings. This results in a supporting system without friction, that do not need lubrication and presents low maintenance cost.

Magnetic Bearings can be classified into two major types: Active Magnetic Bearing (AMB), when there is need to control the circulating current in copper wires of electromagnets, and Passive Magnetic Bearing (PMB), which uses materials like permanent magnets or superconductors.

AMB offers the possibility to identify parameters in real time and to adjust its operation to the working conditions. An appropriate control system, a power stage, as well as good instrumentation are necessary. Because of this, its implementation is costly. In this classification, the so called self-bearing or bearingless motors can also be included [1] [2] [3].

PMB has increased interest on applications with constraints in terms of structure, energy consumption and cost. Among the techniques used are: Diamagnetic (normal temperature), Electrodynamics, Superconducting (diamagnetic at low temperature) and configurations with Permanent Magnets.

The research work using Diamagnetic PMB is directed to micro bearings [4] [5].

The Electrodynamics PMB requires the movement of a magnetic field in the vicinity of a conductive material. The interaction of this magnetic field with the induced currents on the conductive material produces forces of levitation and drag, which depend on the speed of movement [6] [7].

PMB using the diamagnetic property of superconductors developed mainly due to the discovery, by the end of last century, of high critical temperature superconductors (HTS). They present stable levitation due to the partial exclusion of magnetic fields in the proximity of permanent magnets. Energy storage systems of flywheel type [8] and MagLev trains [9] [10] are some applications where they can be found [11].

*elkinrodvel@msn.com, Av. Athos da Silveira Ramos 149, Centro de Tecnologia, I-148. Cidade Universitária, CEP 21941-909 – Rio de Janeiro – Brazil, +552125627873

The use of rare earth magnets in PMB opened opportunities for application in several areas, characterized by a simple framework construction, zero power consumption and low operating cost. Different configurations using two rings of permanent magnet, with axial or radial magnetization, have been suggested in the literature [12] [13], as well as the Halbach array [14], which directs and concentrates the magnetic field. Theoretical analysis and finite element simulations of forces and stiffness have been the subject of studies [15] [16]. The Impeller Left Ventricular Assist Device (LVAD) is an application example [17].
On the other hand, the increasing energy demand drives the improvement in the use and exploitation of energy sources. Renewable energy sources, especially wind, are positioning themselves as an alternative to meet this demand. With the growth of urban centers, the vertical axis wind turbines are presented as a viable and low-cost energy supply, especially for the proper functioning in the presence of turbulent winds and due to the low impact architecture [18] [19]. New families of generators of the vertical axis, for different power levels, are found in the market. Operating improvements can be achieved not only with the aerodynamic design but also with new technologies, as the magnetic suspension.
This paper presents a contribution to the design of passive magnetic bearings for vertical axis wind turbines based on simulations by the Finite Element Method (FEM) and experimental data. For this purpose, two arrangements of magnets will be studied to improve the stability and strength of a radial magnetic bearing. Experimental data will be compared with those obtained by simulations with COMSOL software. The system behavior is analyzed at different operating speeds.

2 Passive Magnetic Bearing

The Passive Magnetic Bearings (PMB) proposed in this paper use two types of ring magnets, that work based on repulsion forces. The geometry and dimensions of these permanent magnets are shown in Figure 1.

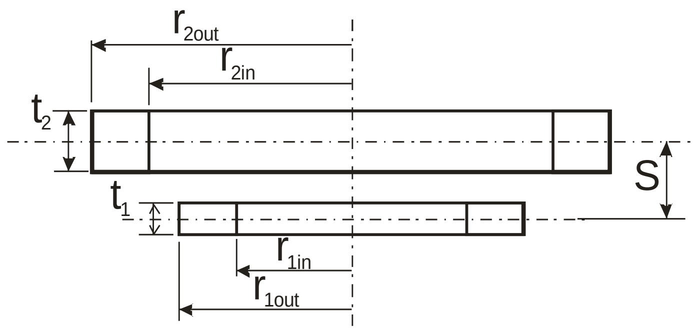

Parameters	Length (mm)	Description
r_{1in}	20	Inner radius of inner ring
r_{1out}	30	Outer radius of inner ring
r_{2in}	35	Inner radius of outer ring
r_{2out}	45	Outer radius of outer ring
S	--	Axial distance from geometric center of each magnet

Figure 1: Ring magnets used for the construction of the proposed Passive Magnetic Bearings

Two PMB configurations were studied:
Figure 2(a) shows the first one with just two permanent-magnetic rings polarized on axial direction with different diameters, which allows inclusion one inside the other.
Figure 2(b) shows the second one, using two opposing magnetic layers [20]. S1 and S2 represent distances from the geometric centers of the inner and outer magnets, respectively.

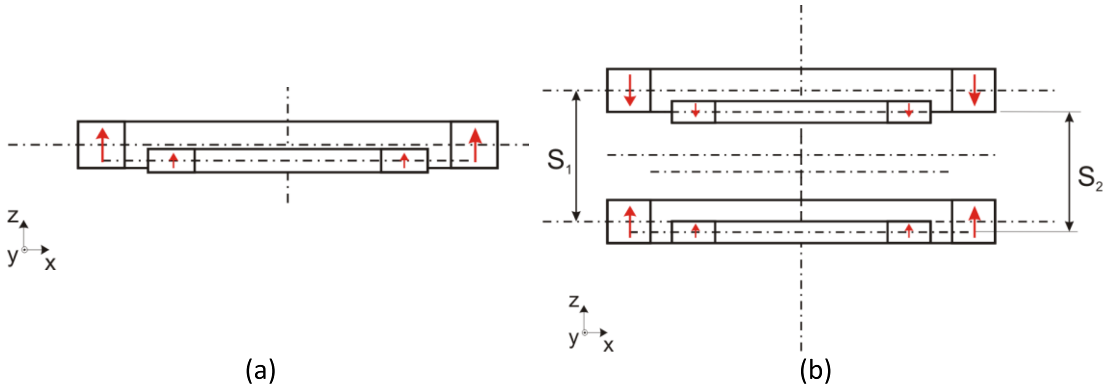

Figure 2: Passive Magnetic Bearing: (a) simplest setup and (b) layered opposing magnet.

2.1 Magnetic field density

The distribution of magnetic field on the surface of each magnet is an important factor for the magnetic-bearing operation, since the geometric center should also be the magnetic center of the prototype, in order to avoid unbalances. Therefore, an analysis of the magnetic field distribution in each magnet is needed for a practical application.

The inner magnets have a magnetic field density up to 0.26 T, and magnetic field distribution as uniform as possible. Figure 3 shows the magnetic field distribution of one internal magnet, measured 1 mm above the upper face, over a 80 x 80 cm surface.

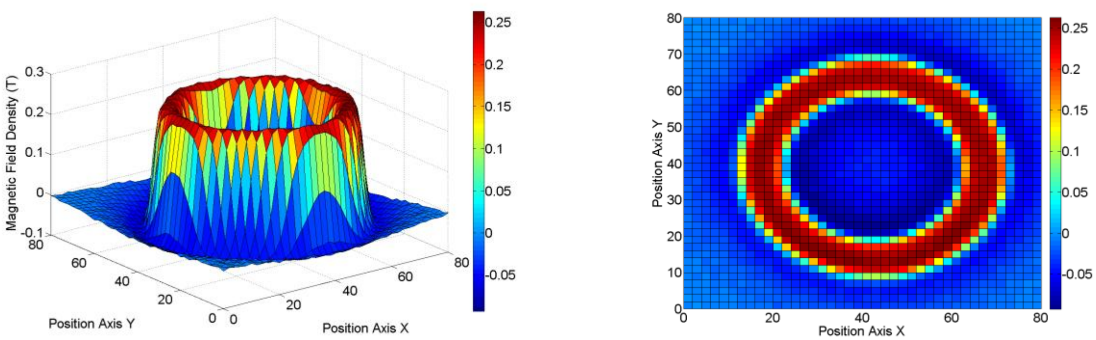

Figure 3: Distribution of magnetic field density of an inner ring.

The outer magnets keep an uniform magnetic field distribution and present 0.37 T as maximal value. Measurements 1 mm above the upper face over a squared-area of 120 x 120 mm are shown in Figure 4. In some magnets, a non-homogeneous magnetic field was found, explaining the oscillations observed experimentally at low speed.

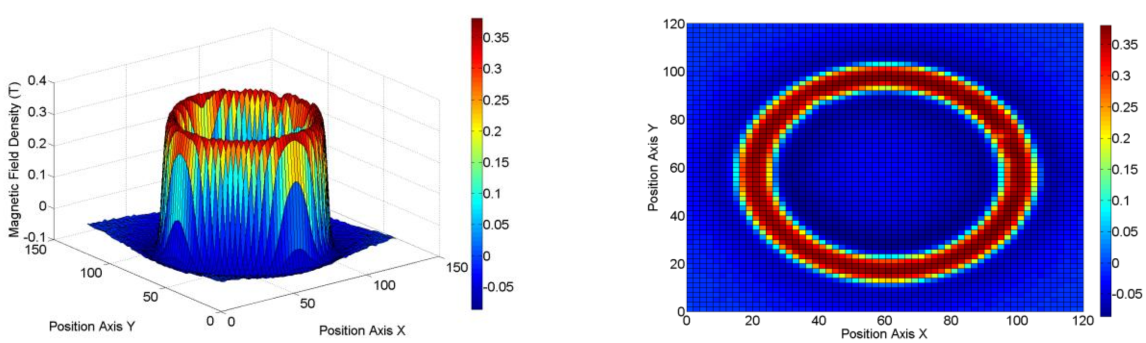

Figure 4: Distribution of magnetic field density of an outer ring.

3 FEM force calculation

In order to evaluate the behavior of forces, simulations were performed using the Finite Element Method (FEM). Both radial and axial forces were calculated whereas the internal magnetic cluster dislocated over X and Z axis. As shown in Figure 2, X axis is transversal to the rotor axis, and Z lies along with the rotor axis. The dimensions of the permanent magnets applied – Nd-Fe-B (N35) – were given in Figure 1. The coercivity force and remanent field are -918 kA/m and 1.198 T, respectively.

3.1 First configuration

Figure 5 presents both axial and radial forces vs. axial and radial displacement for the simplest setup, Figure 2(a). The position “zero” on axis X and Z indicates that the geometric centers of magnets - internal and external - are aligned.
The axial force shows an almost insensitive behavior to radial movements (in direction X). However it increases more evidently whenever it moves from -5 to +5 mm axially (in direction Z) with an unstable behavior. The maximum absolute value is at ±5 mm, Figure 5(a).
In comparison, the radial force shows to be more influenced by both radial and axial movements, Figure 5(b). A linear behavior happens to radial movements (in direction X) and maximum sensibility occurs whilst magnets are geometrically aligned. Radial force is a repulsion force ranging between 6 and -6 mm in the Z axis. Outside this range, it is an attraction force.

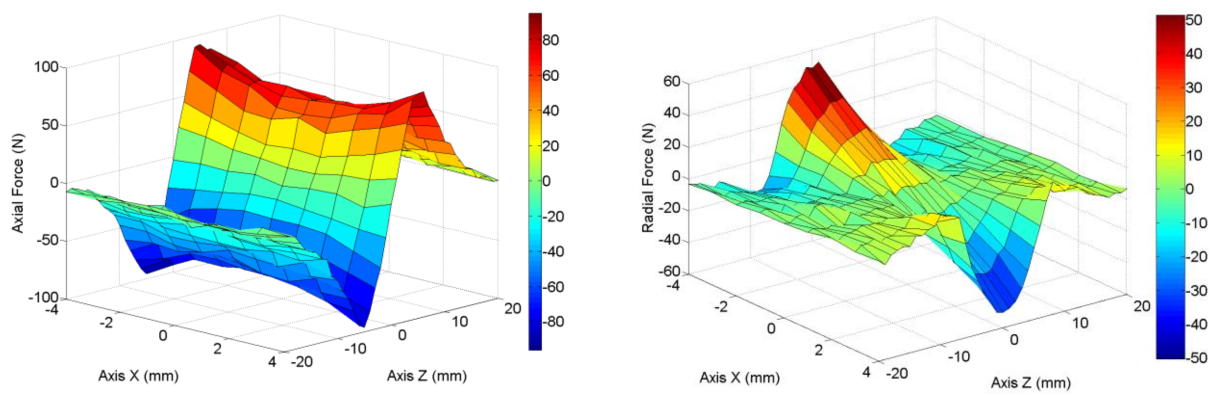

(a) (b)

Figure 5: (a) Axial and (b) radial force for the simplest setup.

3.2 Second configuration

For these simulations, the geometric centers of magnets in Figure 2(b) are considered aligned and S1 = S2 = 23 mm. Figure 6(a) shows the axial force, which presents the same behavior between the range of 5 to -5 mm in comparison to the previous case, Figure 5(a), although its values are increased two-fold. However, the interaction of magnets between 5 and 20 mm leads to a non-linear decrease of force. The radial force is shown in Figure 6(b) and it is similar to the characteristics found in the simplest setup, though two-fold its value.

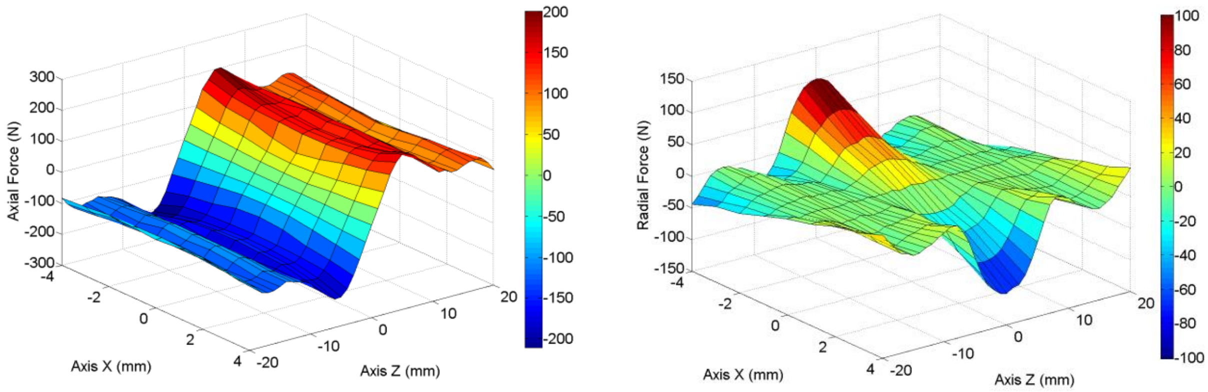

(a) (b)

Figure 6: (a) Axial and (b) radial force to the layered opposing magnet.

These results demonstrate that both radial magnetic bearings present a better behavior when magnets are precisely aligned, thus both geometric and magnetic centers of inner and outer magnets are common. At this point, the best radial stability and lower axial force would be found, although this point is near to the instability margin. According Earshaw´s theorem, the perfect passive magnetic levitation is impossible using only permanent magnets. Locating the inner magnets some millimeters under the outer magnets, the repulsive force directed to the bottom can be compensated for with a foothold,

4 Experimental results

4.1 Static tests

In order to validate the results derived from simulations, two structures to measure axial and radial forces were built on each magnetic bearing, as shown in Figure 7. These tests require a bench composed by a table with a linear actuator located vertically, an ATI load cell [21], and the National Instruments PCI-6040e board.

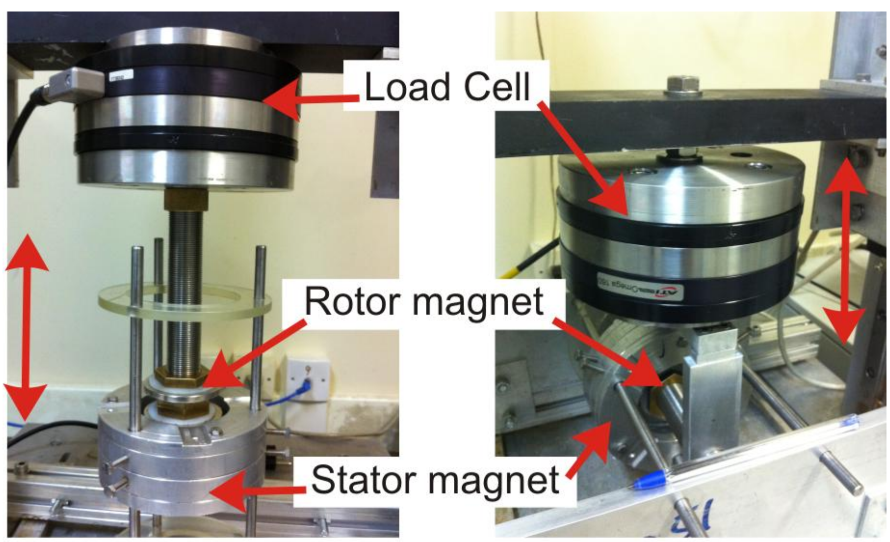

(a) (b)

Figure 7: Measurement system of (a) axial and (b) radial force.

The bench described in Figure 7(a) was used to measure axial force, where there has been a dislocation of 60 mm on the Z axis with steps of 50 µm. Considering its radial force, the bench described in Figure 7(b) was used, performing a 8mm dislocation with a step of 50 µm.

4.1.1 First configuration

The result of radial forces acquired from FEM and experimental data to build up the simplest setup are shown in Figure 8. The graph present similar results, although some data acquired from FEM varied mainly due to mesh quality.

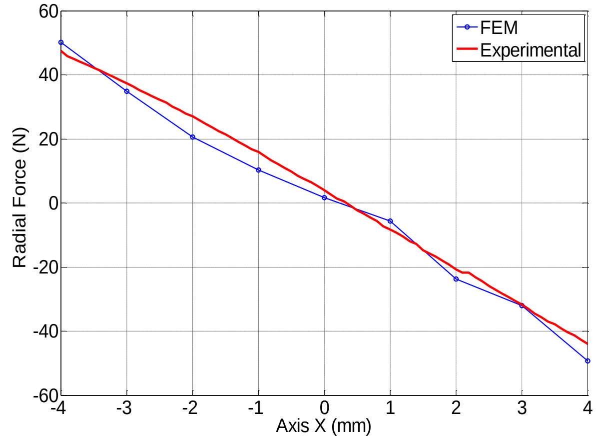

Figure 8: Radial force at the simplest setup.

4.1.2 Second configuration

The results of axial and radial forces acquired with FEM, and experimentally to the layered opposing magnet structure are shown in Figure 9. These results are similar and present the same behavior, thus validating the results obtained with the FEM.

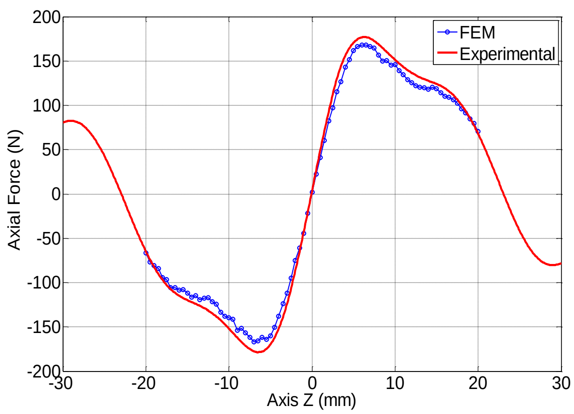

(a)

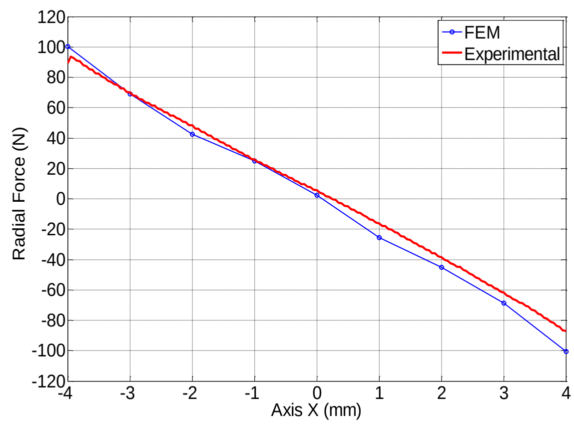

(b)

Figure 9: (a) Axial and (b) radial force at layered opposing magnet.

4.2 Dynamics tests

A top-shaped prototype was built in order to evaluate the dynamic behavior of the passive magnetic bearing (Figure 10). On its base, a teflon piece was applied to reduce mechanical friction. Eddy-current sensors placed on the base measure the position. The velocity was imposed by a motor attached to the prototype by a flexible axis, which offer degrees of freedom to the rotor. The software applied was developed in LabView and the data acquisition was performed by the National Instrument board.

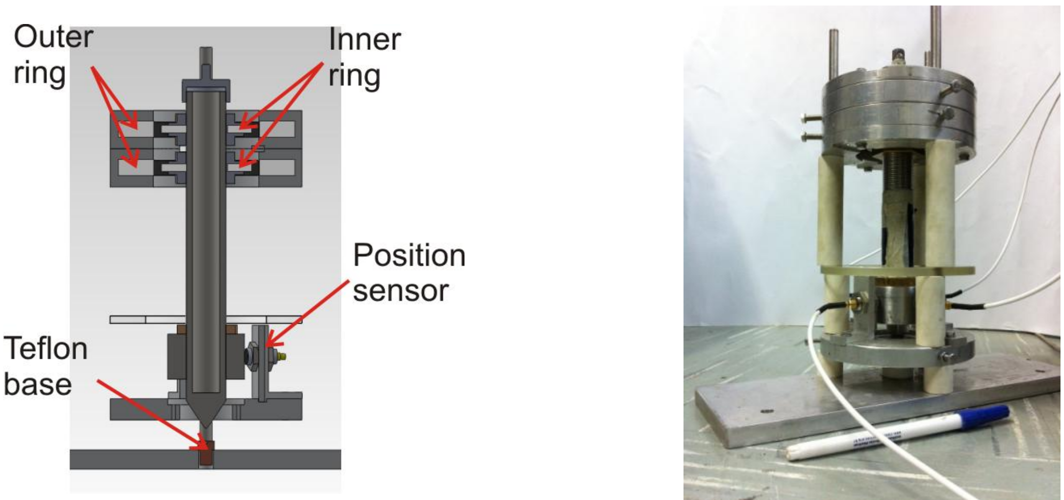

(a) (b)

Figure 10: Passive Magnetic Bearing prototype, (a) cross section and (b) photo.

4.2.1 First configuration

The geometric center of the outer magnet was positioned 186.2 mm from the teflon base, approximately. The geometric center of the inner magnet lies around 2 mm under the geometric center of the outer magnet. The radial bearing was tested also at different speeds. Figure 11 shows a XY graphic, which indicates some displacement of the rotor to 60, 800, 1200, 1800 and 2300 rpm. The displacement average peak-to-peak of the rotor vs. speed is shown in Figure 12.

As observed, the displacement averages in both axes are lower than 1mm in the speed ranges from 0 to 800 rpm and above 1600 rpm. The resonant speed appears in the range 800 – 1600 rpm and is 1190 rpm, approximately. The amplitude in Y-axis is greater than that in X-axis.

4.2.2 Second configuration

The structure of layered opposing magnet was also tested (Figure 2(b)). The geometric center of both external magnets was approximately 186.2 mm from the teflon base, equal to simplest setup. On the other hand, the geometric center of inner magnets was 2 mm under the center of outer magnets, then keeping a 2 mm distance between outer and inner magnets. It maintains a good performance of radial and axial forces, avoiding destabilization due to little perturbations on the bearing system. Figure 13 shows the radial orbit of the rotor in XY graphics for 60, 800, 1600, 1900 and 2400 rpm. The displacement average peak-to-peak of the rotor vs. speed is shown in Figure 14.

The displacement average of the both axes is lower than in the first case. The resonant frequency changed to 1600 rpm.

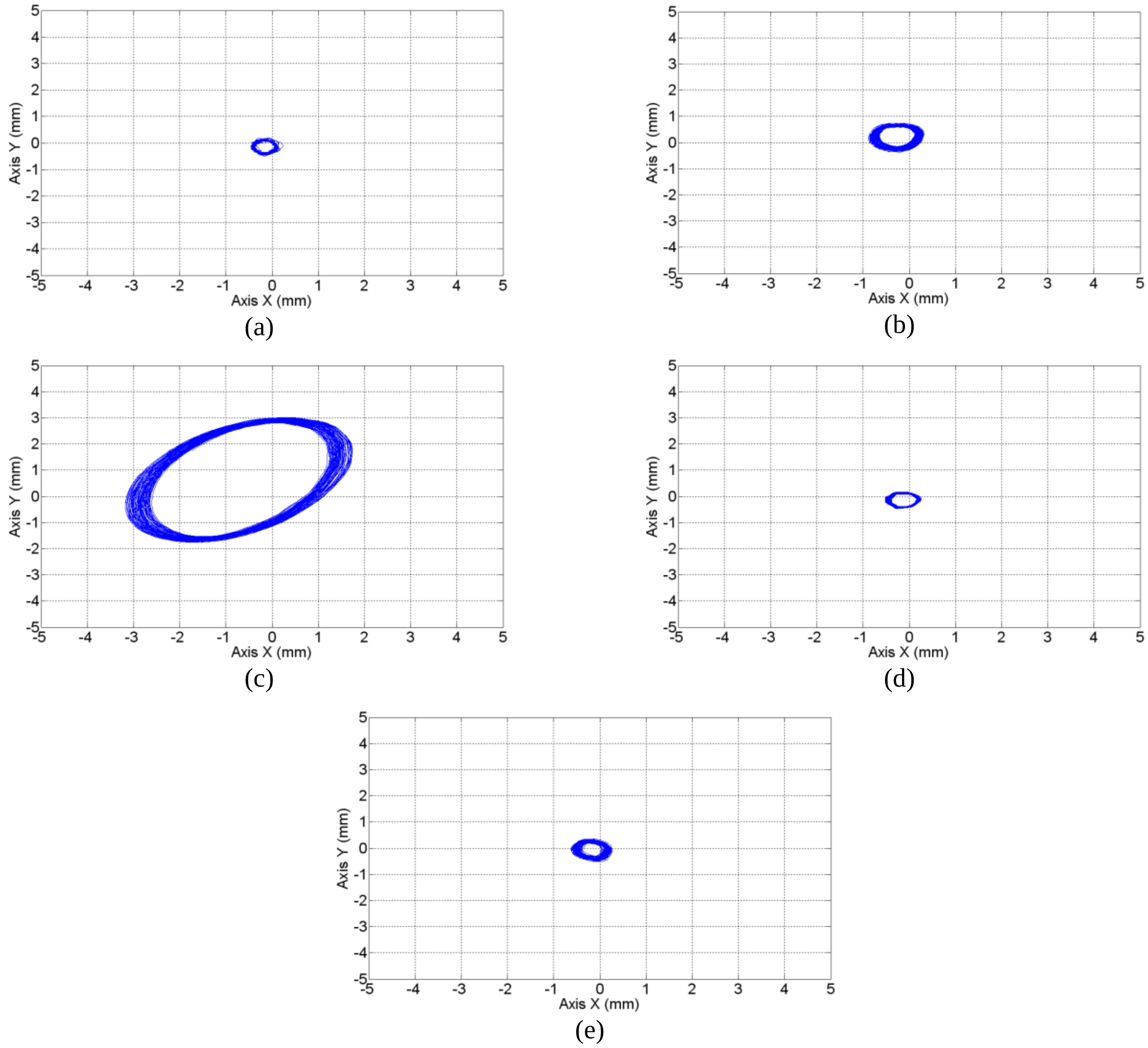

Figure 11: Radial orbit of the bearing simplest setup for (a) 60, (b) 800, (c) 1200, (d) 1800 and (e) 2300 rpm.

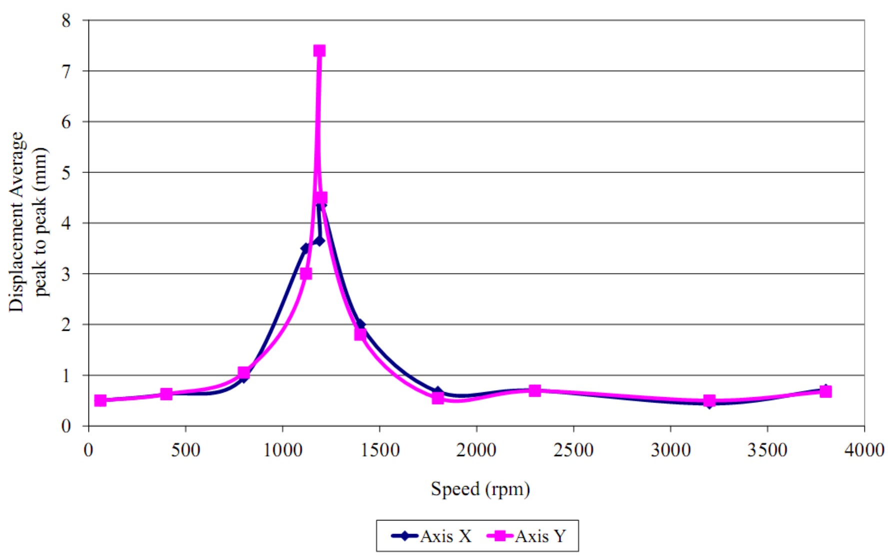

Figure 12: Behavior of rotor position due to velocity changes for the simplest setup.

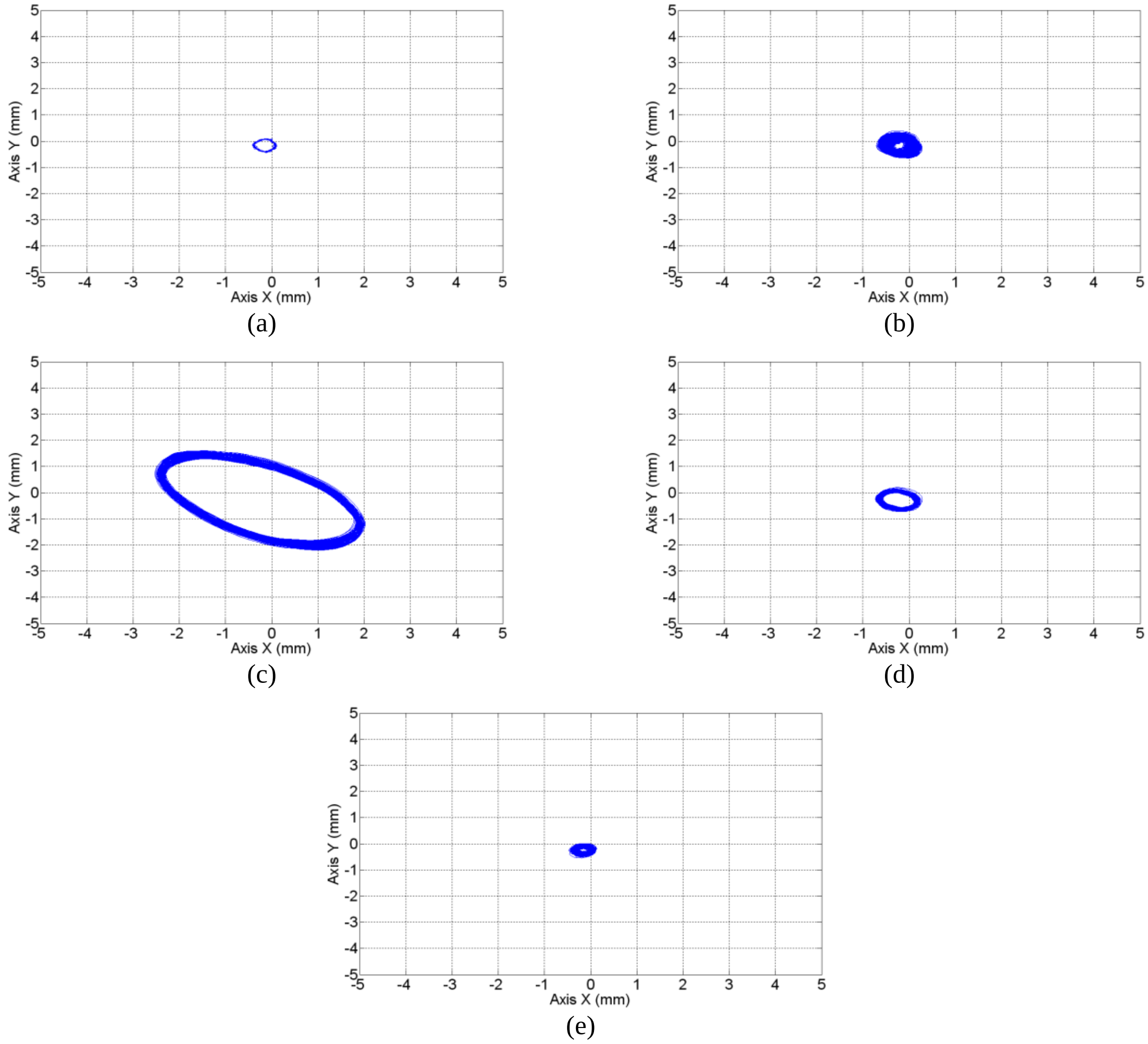

Figure 13: Radial orbit of the bearing layered opposing magnet for (a) 60, (b) 800, (c) 1600, (d) 1900 and (e) 2400 rpm.

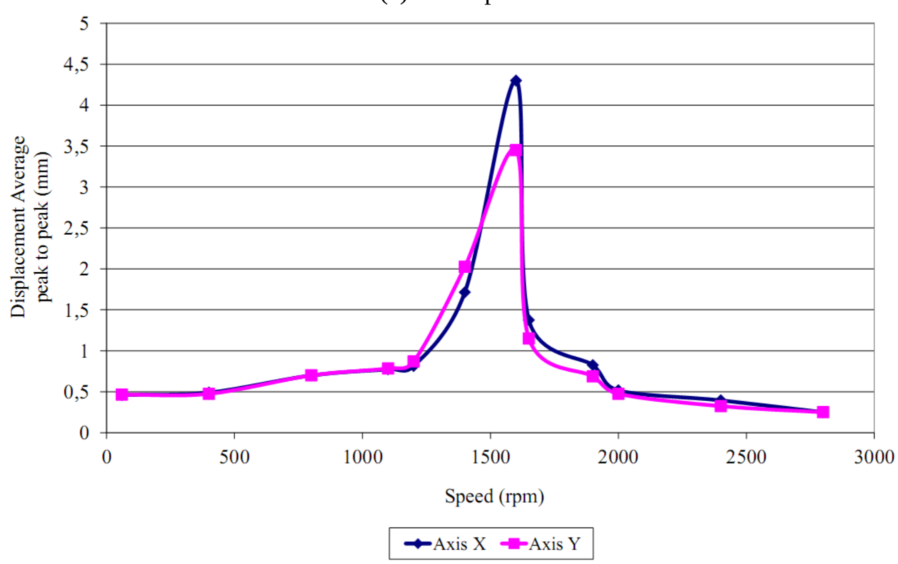

Figure 14: Behavior of the rotor position due to velocity changes at the layered opposing magnet.

5 Conclusion

This research work presented the static and dynamic performance of two passive magnetic bearings for vertical axis operation aiming the application in wind turbines. The double layered bearing showed a better behavior, both for static and dynamic situations.

In any case, a resonance frequency exists and must be taken into account for the successful implementation of the proposed magnetic suspension.

The simulation results match with the experimental ones, giving confidence for further designs based only on simulation studies.

The next step of this research will investigate an optimal configuration following the procedure proposed in [22]. The results will be used for the construction of a small scale vertical axis wind turbine.

6 Acknowledgments

The authors would like to thank the financial support of FAPERJ and the mechanical design and construction made by Eng. Felipe Costa and Mr. Genésio Santanna.

References

[1] G. Schweitzer et al., *Magnetic Bearings: Theory, design and application to rotating machinery*, Springer Verlag, 2009.

[2] A. Chiba, et al., *Magnetic Bearings and Bearingless Drives*, Elsevier, Great Britain, 2005, ISBN 0 7506 5727 8.

[3] E. F. Rodriguez, J. A. Santisteban, *An improved control system for a split windings bearingless induction motor*, IEEE Transactions on Industrial Electronics, volume 58, issue 8, pp 3401-3408, 2011.

[4] A. Cansiz and J. R. Hull, *Stable Load-Carrying and Rotational Loss Characteristics of Diamagnetic Bearings*, IEEE Transactions on Magnetics, Vol. 40, No. 3, May 2004.

[5] Jie-Yu Chen, et al., *Evaluation of Eddy-Current Effects on Diamagnetic Bearings for Microsystems*, IEEE Transactions on Industrial Electronics, Vol. 56, No. 4, April 2009.

[6] J. L. He, D, M. Rote, and H. T. Coffey, *Study of Japonese Electrodynamic – Suspension Maglev Systems*. Center for Transportation Research Argonne National Laboratory, 1994.

[7] M. T. Tompson, *Eddy Current Magnetic Levitation – Models and Experiments*, IEEE Potentials, pp. 40-44, 2000.

[8] G. G. Sotelo, et al., *Halbach array superconducting Magnetic Bearing for a flywheel energy storage system*, IEEE Transactions on Applied Superconductivity, Vol 15, No. 2, pp 2253-2256, June 2005.

[9] R. M. Stephan, et al., *Levitation force and stability of superconducting linear bearings using NdFeB and ferrite magnets*, Physica C: Superconductivity, Volume 386, pp 490–494, 15 April 2003.

[10] G. G. Sotelo, et al., *Experimental and Theoretical Levitation Forces in a Superconducting Bearing for a Real-Scale Maglev System*, IEEE transactions on applied superconductivity, Vol. 21, No. 5, October 2011.

[11] F. N. Werfel, et al., *HTS Magnetic Bearings in prototype application*, IEEE Transactions on applied superconductivity, Vol. 20, No. 3, June 2010.

[12] Jean-Paul Yonnet, *Passive Magnetic Bearings with permanent magnets*, IEEE Transactions on Magnetics, Vol. MAG-14, No. 5, September 1978.

[13] J. Delamare, E. Rulliere and J. P. Yonnet, *Classification and sybthesis of permanent magnet bearing configurations*, IEEE Transactions on Magnetics, Vol 31, pp 4190-4192, 1995.

[14] Xu Feipeng, Li Tiecai and Lui Yajing, *A study on passive magnetic bearing with Halbach magnetized array*, International Conference on Electrical Machines and Systems, ICEMS 2008, pp 417-420, 2008.

[15] R. Ravaud, G. Lemarquand and V. Lemarquand, *Force and stiffness of Passive Magnetic Bearings using permanent Magnets. Part 1: Axial Magnetization*, IEEE Transactions on Magnetics, Vol. 45, No. 7, July 2009.

[16] R. Ravaud, G. Lemarquand and V. Lemarquand, *Force and stiffness of Passive Magnetic Bearings using permanent Magnets. Part 2: Radial Magnetization*, IEEE Transactions on Magnetics, Vol. 45, No. 9, September 2009.

[17] K. Qian, Z. Xu and H. Wang, *Investigation on applying Passive Magnetic Bearings to impeller left ventricular assist devices (LVAD)*, 3rd International Conference on Biomedical Engineering and Informatics – BMEI 2010.
[18] G. Müller, M. F. Jentsch and E. Stoddart, *Vertical axis resistance type wind turbines for use in buildings*, ELSEVIER, Renewable energy 34, pp. 1407-1412, 2009.
[19] T. Bertényi and T. Young, *Power Electronics solutions for vertical axis urban wind turbines*, IEEE Electrical Power & Energy Conference, 2009.
[20] R. Moser, J Sandtner and H. Bleuler, *Optimization of repulsive passive magnetic bearings*, IEEE Transactions on magnetic, Vol. 42, No. 8, August 2006.
[21] ATI Industrial Automation, *Compilation of Manuals*, Engineered products for robotic productivity, Document #: 9610-05-1022, 2011.
[22] E. S. Motta, et al., *Optimization of a linear superconducting levitation system*, IEEE Transactions on applied superconductivity, Vol 21, No. 5, October 2011.